Training Course
FIELD CALIBRATION OF IRRIGATION STRUCTURES
Fordwah Canal
Fordwah Eastern Sadiqia Irrigation and Drainage Project

Bahawalnagar, 28 May to 6 June, 1995

Technical Report

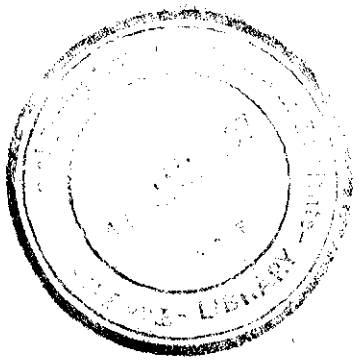

Maqbool Ahmad
Barkat Ali
Salamat Ali
M. Aslam
Qamar Rasool Babar
M. Shabbir Haider
Khadim Hussein
Shahid Iftikhar
Anwar Iqbal
Mushtaq Ahmed Khan
Marcel Kuper
Khalid Mehmood
M. Ali Pasha
M. Ramzan
Rana Akhtar Raza
Abdul Razaq
Akhtar Riaz
Abdul Samad
Qasim Ali Shah
Ghulam Rasool Shauq
Gaylord Skogerboe

Lahore

August 1995

TABLE OF CONTENTS

PAGE

Part 1

CHAPTER 1:Introduction 1

1.1. Background 1
1.2. Description of the System 2
1.3. Units 2

CHAPTER 2: Methodology-Hydraulic principles rating of structures 3

2.1. Backwater Effects 3
2.2. Free-Flow and Submerged-Flow 3
2.3. Rating Open Channel Constrictions 7
2.3.1 Free Flow 7
2.4. Rating Orifices 23
2.4.1 Free-Flow Rectangular Gate Structures 25
2.4.2 Submerged-Flow Rectangular Gate Structures 33
2.4.3 Calibrating Large Gate Structures 39
2.5. Current Meters for Discharge Measurement 43
2.5.1 Types of Current Meters 43
2.5.2 Care of Equipment 45
2.5.3 Current Meter Ratings 45
2.6. Methods of Emplying Current Meters 47
2.6.1 Wading 47
2.6.2 Bridge 47
2.6.3 Cableway 48
2.6.4 Boat 48
2.7. Velocity Measurement Methodologies 48
2.7.1 Vertical Velocity Method 48
2.7.2 Two Points Method 49
2.7.3 Six-Tenths Depth Method 49
2.8. Velocity at Vertical Walls 50
2.9. Selection of Measuring Cross-Section 50
2.10. Subdivision of Cross-Section into Verticals 52
2.11. Measurement of Water Depths 52
2.12. Recording of Data 52
2.13. Unsteady Flow Conditions 55
2.14. Computational Procedure 55

PAGE

CHAPTER 3: Results - Rating of Structures 62

3.1. Physical characteristics of structures 62
3.2. ISRIP Calibration 66
3.3. IIMI-ID Calibration 67
3.4. Rating Structures with $KD^{5/3}$ formula 69

CHAPTER 4: Methodology: Inflow-Outflow Test 72

CHAPTER 5: Results: Inflow-Outflow Test 74

Recommendations field calibration training course 77

Acknowledgements 78

Part 2 : Training Reports 79

1.1. Report No. 1 79
1.2. Report No. 2 81
1.3. Report No. 3 83

Annex 1 List of participants 86

Annex 2 Programme of the Training Course 87

Annex 3 Team Composition and Training Inflow-Outflow Test 90

Annex 4 Data Sets - Specimen attached 92

CHAPTER 1: Introduction

1.1. Background

IIMI was asked in 1989 by the Secretaries of Irrigation & Power and Agriculture of the Government of Punjab to commence work in the Fordwah/Eastern Sadiqia area, given the fact that a number of development projects would be initiated in the area. The objective of IIMI's research is to develop and pilot test in collaboration with national research and line agencies *alternative irrigation management practices to optimize agricultural production and mitigate problems of salinity/sodicity*. The research is carried out at various levels of the irrigation system, from main system operations to field level irrigation application.

The main system component of the research is carried out in collaboration with the Punjab Irrigation & Power Department and aims to develop tools to assist irrigation managers to take better founded decisions on operations and maintenance. Within the framework of this programme, a field calibration training course was organized in the Fordwah Canal Division on the request of the Secretary Irrigation & Power Department, Punjab.

The training course had four main components:

1. Classroom and field site lectures on hydraulic principles of rating of structures and the use of the current meter

2. Rating of distributary head regulators by current meter (wading method)

3. Inflow-outflow test to determine seepage losses

4. Rating of major structures and cross-regulators by current meter (suspension method, boat)

The participants of the training course calibrated all hydraulic structures of the Chishtian sub-division (Fordwah Branch RD 199-371). Upon completion of the rating of structures (component 2), an inflow-outflow test was conducted to estimate the seepage losses in Fordwah Branch (RD 199-371). Finally, component 4 was entrusted to the International Sedimentation Research Institute, Pakistan (ISRIP). The training course was organized from 28 May to 6 June in Bahawalnagar.

Limitations

To develop the rating of hydraulic structures, measurements have to be taken with a range of discharges (e.g. 20%, 40%, 60%, 80%, 100% and 120% of the full supply discharge). Thus, the training course was organized during a period in which supplies were not at their maximum. During this ten-day period, 1-2 measurements were taken for each structure. Although this will give a good idea of the rating of these structures, more measurements will be required to develop full rating curves.

1.2. Description of the System

Fordwah canal off-takes from the left abutment of Suleimanki Headworks on the Sutlej river and conveys water to MacLeod Ganj and Fordwah Branch canals at its tail at RD 44850 (see map). Fordwah Branch canal runs for about 75 miles (tail RD is 371650) and has a full supply discharge of 2603 cusecs. The head of the system is non-perennial and receives supplies from 15 April to 15 October only. At RD 129 of Fordwah Branch, the Sadiq-Ford feeder supplies water to Fordwah Branch from 15 October to 15 April in order to feed the perennial canals of the Fordwah system. The Fordwah Division is divided into three sub-divisions, Minchinabad (from the head of Fordwah canal to RD 77 of Fordwah Branch), Bahawalnagar (from RD 77 to RD 199 of the Fordwah Branch) and Chishtian (from RD 199 to 371 of Fordwah Branch). See the index plan on the next page.

1.3. Units

During the training course the participants were trained to convert easily from the metric system to the imperial system and back. Although the metric system has been officially adopted in Pakistan, imperial units are very much in use in Pakistan's irrigation system. It is for this reason that while the units in the more generic cheapter 2 on methodology are kept in the metric system, units in the results chapter are presented in the imperial system. Conversions are given in the table below for an easy reference of the reader.

Conversion Factors

1 foot (= 12 inches)	0.3048 m = 30.48 cm
1 foot/second	0.3048 m/s
1 (cubic) foot/second (cusec)	0.0283 m^3/s = 28.3 l/s
1 metre (=100 cm)	3.28 feet
1 m/s	3.28 feet/s
1 m^3/s (cumec) (=1000 l/s)	35.31 cusec

INDEX PLAN OF FORDWAH DIVISION

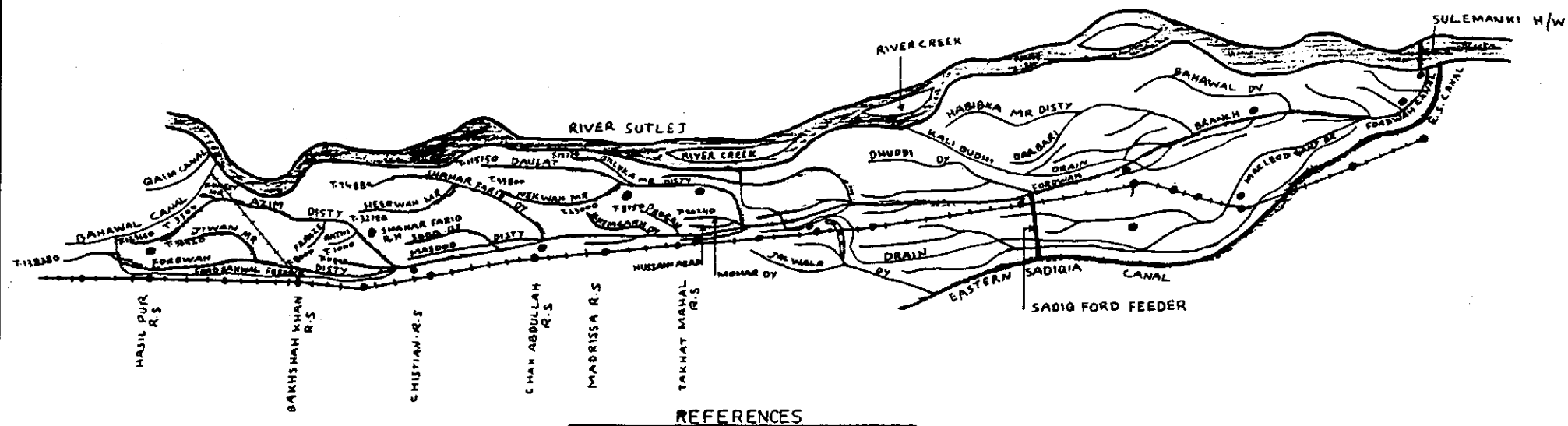

REFERENCES

1. RIVER	
2. CHANNELS	
3. REST HOUSE	
4. RAILWAY LINE	
5. DRAINS	
6. FLOOD PROTECTION BUND	

CHAPTER 2: Methodology - Hydraulic principles rating of structures[1]

2.1. Backwater Effects

A simple open-channel constriction is shown in Figure 1. The flow through such constrictions is most often in the tranquil range, and produces gradually varied flow far upstream and a short distance downstream, although rapidly varied flow occurs at the constriction (Barrett and Skogerboe 1973). The effect of the constriction on the water surface profile, both upstream and downstream, is conveniently measured with respect to the normal water surface profile, which is the water surface in the absence of the constriction under uniform flow conditions. Upstream of the constriction, an "M1" or "M2" backwater profile occurs. The maximum backwater effect, denoted by y* in Figure 1, occurs a relatively short distance upstream. The backwater effect may extend for a considerable distance in the upstream direction, particularly for irrigation channels with flat longitudinal gradients. Immediately downstream of the constriction, the flow expansion process begins and continues until the normal regime of flow has been re-established in the channel.

2.2 Free-Flow and Submerged-Flow

The two most significant flow regimes under which any open channel constriction may operate are free-flow and submerged-flow. Other terms for free-flow are critical-depth flow and modular flow, while other terms for submerged-flow are drowned flow and non-modular flow. The distinguishing difference between the two flow conditions is the occurrence of critical velocity in the vicinity of the constriction (usually a very short distance upstream of the narrowest portion of the constriction). When this critical flow control occurs, the discharge is uniquely related to the depth of "head" upstream of the critical section. Thus, measurement of a flow depth at some specified location upstream, h_u, from the point of the critical conditions is all that is necessary to obtain the free-flow discharge, Q_f. Consequently, Q_f can be expressed as a function of h_u:

$$Q_f = f(h_u) \qquad (1)$$

When the flow conditions are such that the downstream flow depth is raised to the extent that the flow velocity at every point through the constriction becomes less than the critical value, then the constriction is operating under submerged-flow conditions. With this flow regime, an increase in tailwater flow depth, Δh_d, will increase the head upstream of the constriction by Δh_u (Δh_u will be less than Δh_d). Both the upstream depth, h_u, and the downstream depth, h_d, must be measured to determine the discharge through a calibrated constriction operating under submerged-flow conditions.

---

[1] The material of this Chapter was taken from a manual by the same title published by the International Irrigation Center, Utah State University dated January 1992 and authored by Gaylord V. Skogerboe, Gary P. Merkley, M.S. Shafique and Carlos A. Gandarillas.

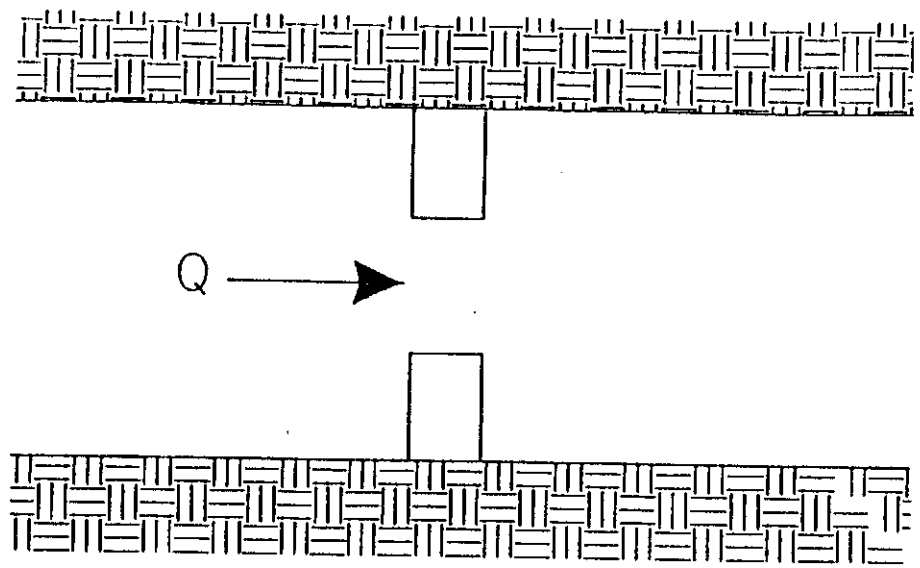

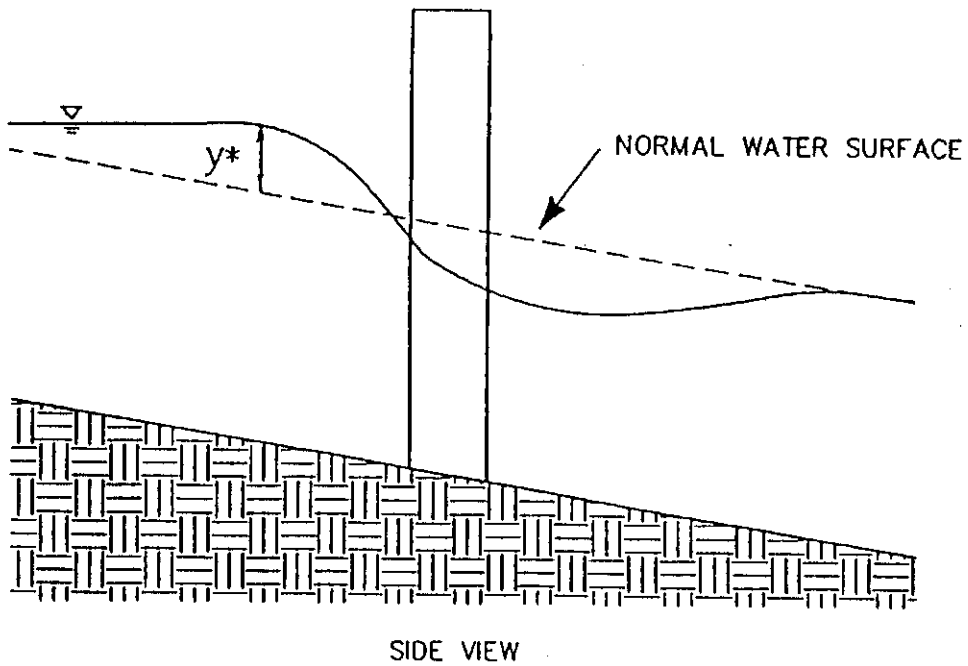

Figure 1. Definition sketch for backwater effects from an open-channel constriction.

The definition given to submergence, S, is:

$$S = \frac{h_d}{h_u} \tag{2}$$

The submergence may also be represented in percent. The submerged-flow discharge, Q_s, is a function of h_u and h_d and the governing relationship is generally written in terms of discharge, head loss (h_u - h_d), and submergence:

$$Q_s = f(h_u, h_d) = f(h_u - h_d, S) \tag{3}$$

Ofttimes, constrictions designed initially to operate under free-flow conditions become submerged as a result of unusual operating conditions, or the accumulation of moss and vegetation in the open channel. Care should always be taken to note the operating condition of the constriction in order to determine which rating should be used. The value of submergence marking the change from free-flow to submerged-flow, or vice versa, is referred to as the transition submergence, S_t. At this condition, the discharge given by the free-flow equation is exactly the same as that given by the submerged-flow equation. Hence, if discharge equations are known for both free-flow and submerged-flow conditions, a definite value of the transition submergence can be obtained by setting the equations equal to one another and solving for S_t. It should be noted that this derived value of S_t is highly sensitive to slight errors in the coefficients or exponents of either equation (Skogerboe, Hyatt and Eggleston 1967).

The difference between free-flow, the transition state, and submerged-flow water surface profiles is illustrated for a simple channel constriction in Figure 2. Water surface profile (a) illustrates free-flow, and (b) indicates the transition submergence condition. Both profiles (a) and (b) have the same upstream depth, with profile (b) having the maximum submergence value for which the free-flow condition can exist. The submerged-flow condition is illustrated by profile (c), where an increase in the tailwater depth has also increased the depth of flow at the upstream station.

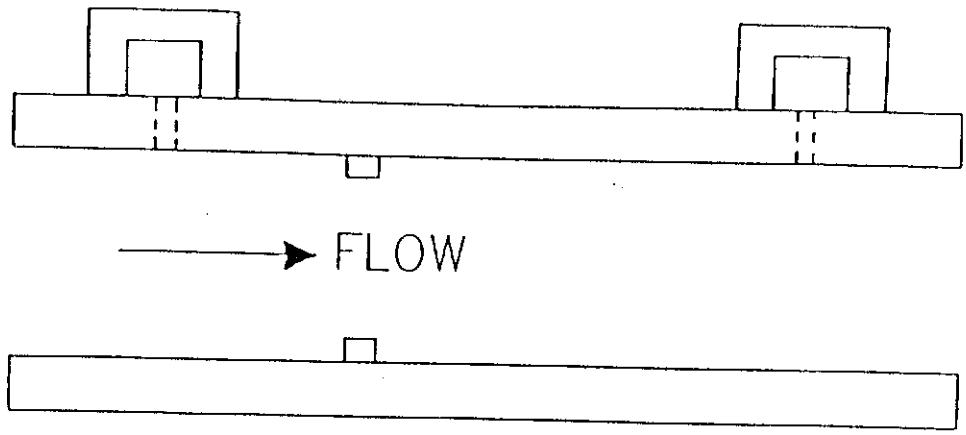

PLAN VIEW

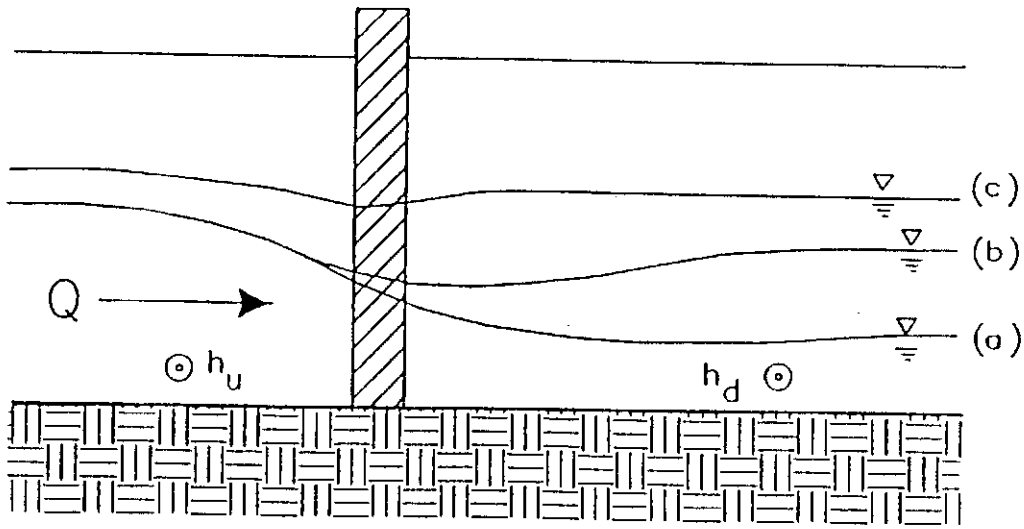

SIDE VIEW

Figure 2. Illustration of flow conditions in an open-channel constriction.

2.3 Rating Open Channel Constrictions

2.3.1 Free Flow

The general form of the free-flow equation is:

$$Q_f = C_f h_u^{n_f} \quad (4)$$

where the subscript f denotes free flow, so that Q_f is the free-flow discharge, C_f is the free-flow coefficient, and n_f is the free-flow exponent. The value of C_f increases as the size of the constriction increases, but the relationship is usually not linear. The value of n_f is primarily dependent upon the geometry of the constriction with the theoretical values being 3/2 for a rectangular constriction and 5/2 for a triangular constriction. A trapezoidal constriction would have a free-flow exponent of 3/2 at extremely shallow flow depths and 5/2 for extremely deep flow depths; thus, n_f increases with depth at a trapezoidal constriction. The theoretical values of n_f are modified by the approach velocity, so that n_f increases as the approach velocity increases. However, the measured values correspond very well with the theoretical values for very low approach velocities.

A hypothetical example of developing the field discharge rating for a rectangular open-channel constriction is illustrated in Figure 3, and the field data is listed in Table 1. The discharge rate in the constriction was determined by taking current meter readings at a location upstream, and again at another location downstream. This is a good practice because the flow depths upstream and downstream are often significantly different, so that the variation in the measured discharge between the two locations is indicative of the accuracy of the current meter equipment and the methodology used by the field staff.

A logarithmic plot of the free-flow data (see Table 2) is shown in Figure 4 for the stilling well flow depths, $(h_u)_{sw}$. Note that n_f is the slope of the straight line and C_f is the value of Q_f for $(h_u)_{sw} = 1.0$, since

$$Q_f = C_f(1.0)^{n_f} = C_f \quad (5)$$

The slope, n_f, must be determined using a scale as illustrated. The resulting free-flow equation is:

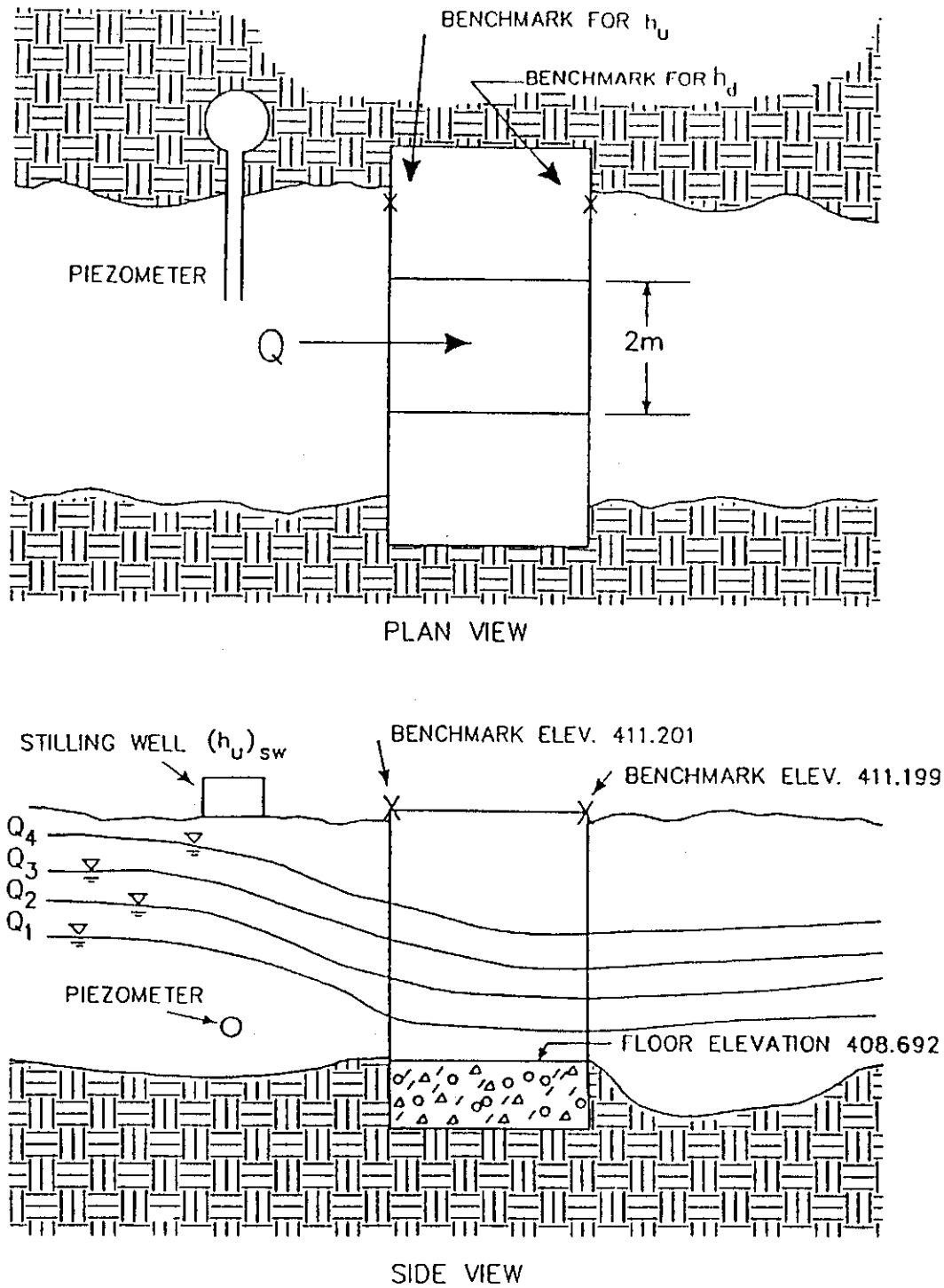

Figure 3 Example of free flow water surface profiles for an open-channel constriction.

TABLE 1. Free-flow field data for example open-channel constriction.

Date	Discharge m^3/s	Water Surface Elevation in Stilling Well, m	Tape Measurement from Benchmark, m
21 Jun 86	0.628	409.610	1.604
21 Jun 86	1.012	409.935	1.294
21 Jun 86	1.798	410.508	0.734
21 Jun 86	2.409	410.899	0.358

Note: The listed discharge is the average discharge measured with a current meter at a location 23 m upstream of the constriction, and at another location 108 m downstream.

TABLE 2. Free-flow data reduction for example open-channel constriction.

Discharge m^3/s	Water Surface Elevation, m	$(h_u)_{sw}$ m	Tape Measurement m	$(h_u)_x$ m
0.628	409.610	0.918	1.604	0.905
1.009	409.935	1.243	1.294	1.215
1.797	410.508	1.816	0.734	1.775
2.412	410.899	2.207	0.358	2.151

Note: The third column values equal the values in the second column minus the floor elevation of 408.692 m. The values in the last column equal the benchmark elevation of 411.201 m minus the floor elevation of 408.692 m minus the values in column four.

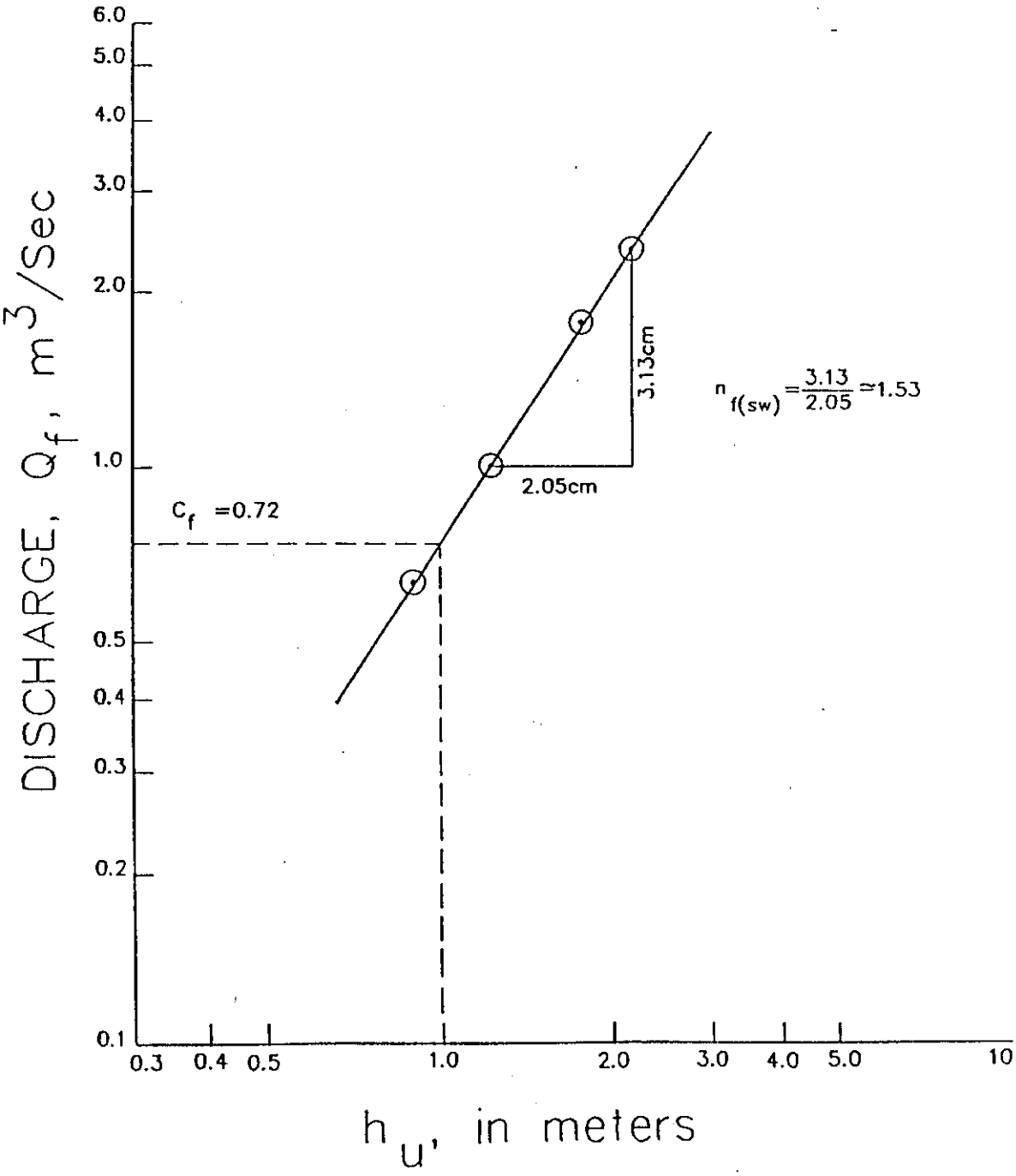

Figure 4. Free-flow discharge rating using the example data.

$$Q_f = 0.72 (h_u)_{sw}^{1.53} \quad (6)$$

A comparison of the free-flow ratings for the stilling well flow depths (Equation 6) and the flow depths along the headwall measured from the benchmark are shown in Figure 5. The free-flow equation for the flow depths measured below the benchmark is:

$$Q_f = 0.74 (h_u)_{sw}^{1.55} \quad (7)$$

If a regression analysis is done with the free-flow data using the theoretical value on $n_f = 3/2$,

$$Q_f = 0.73 (h_u)_{sw}^{1.5} \quad (8)$$

$$Q_f = 0.75 (h_u)_{x}^{1.5} \quad (9)$$

A comparison of Equations 6 and 8 and Equations 7 and 9 are shown in Table 3. The discharge error resulting from using $n_f = 3/2$ varies from -1.91 percent to +2.87 percent.

2.3.2 Submerged Flow

The general form of the submerged-flow equation is:

$$Q_s = \frac{C_s (h_u - h_d)^{n_f}}{(-\log S)^{n_s}} \quad (10)$$

Where the subscript s denotes submerged flow, so that Q_s is the submerged-flow discharge, C_s is the submerged-flow coefficient, and n_s is the submerged-flow exponent. Note that the free-flow exponent, n_f, is used with the term $h_u - h_d$. Consequently, n_f is determined from the free-flow rating, while C_s and n_s is between 1.0 and 1.5 (Skogerboe and Hyatt 1967).

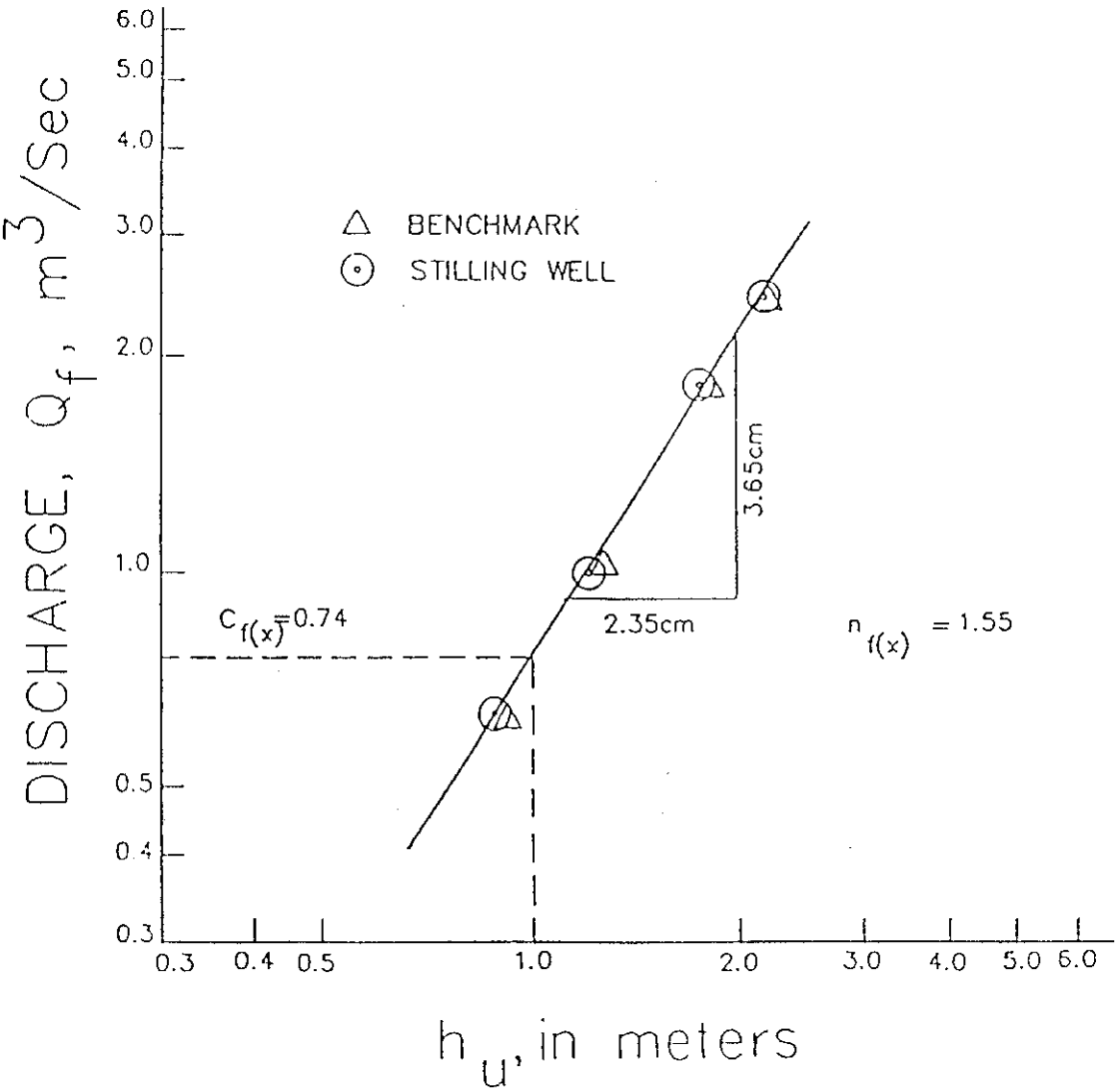

Figure 5. Comparison of free-flow discharge ratings for stilling well and benchmark flow depths.

TABLE 3. Errors in discharge ratings assuming $n_f = 1.5$ for the example rectangular open-channel constriction.

Measured Discharge m^3/s	Measured Depth, $(h_u)_{sw}$ m	$Q_f=0.72(h_u)_{sw}^{1.53}$ m^3/s	Percent Error	$Q_f=0.73(h_u)_{sw}^{1.50}$ m^3/s	Percent Error
0.628	0.918	0.632	0.64	0.642	2.23
1.009	1.243	1.004	-0.50	1.012	0.30
1.797	1.816	1.794	-0.17	1.786	-0.61
2.412	2.207	2.417	0.21	2.393	-0.80

Measured Discharge m^3/s	Measured Depth, $(h_u)_x$ m	$Q_f=0.74(h_u)_x^{1.55}$ m^3/s	Percent Error	$Q_f=0.75(h_u)_x^{1.50}$ m^3/s	Percent Error
0.628	0.905	0.634	0.96	0.646	2.87
1.009	1.215	1.001	-0.79	1.004	-0.50
1.797	1.775	1.801	-0.22	1.774	-1.28
2.412	2.151	2.426	0.58	2.366	-1.91

The value of the free-flow exponent, n_f, can also be determined through an iterative procedure from only submerged-flow data. An initial value for n_f can be assumed (e.g. the theoretical value), then repeatedly adjusted as the approximating submerged-flow equation better fits the field or laboratory data. Such a procedure may be necessary when a constriction is to be calibrated in the field and only operates under submerged-flow conditions. This procedure is best applied using a programmable calculator or computer, in which case the solution can be obtained rapidly.

The hypothetical example illustrated in Figure 3 will be used to demonstrate the procedure for developing the submerged-flow discharge rating. The two benchmarks shown in Figure 3 will be used for measuring h_u and h_d. In this case, a constant discharge was diverted into the irrigation channel and a check structure with gates located 120 m downstream was used to continually increase the flow depths. Each time that the gates were changed, it took 2-3 hours for the water surface elevations upstream to stabilize. Thus, it took one day to collect the data for a single discharge rate. The data listed in Table 4 was collected in two consecutive days. The data reduction is listed in Table 5.

TABLE 4. Submerged-flow field data for example open-channel constriction.

Date	Discharge m^3/s	Tape Measurement from U/S Benchmark	Tape Measurement from D/S Benchmark
22. Jun 86	0.813	1.448	1.675
22 Jun 86	0.823	1.434	1.605
22 Jun 86	0.825	1.418	1.548
22 Jun 86	0.824	1.390	1.479
23 Jun 86	0.793	1.335	1.376
23 Jun 86	1.427	0.983	1.302
23 Jun 86	1.436	0.966	1.197
23 Jun 86	1.418	0.945	1.100
23 Jun 86	1.377	0.914	1.009
23 Jun 86	1.241	0.871	0.910

TABLE 5. Submerged-flow data reduction for example open-channel constriction.

Q_s m^3/s	$(h_u)_x$ m	$(h_d)_x$ m	S	-log S	$Q\Delta_h=1$
0.813	1.061	0.832	0.784	0.1057	7.986
0.823	1.075	0.902	0.839	0.0762	12.486
0.825	1.091	0.959	0.879	0.0560	19.036
0.824	1.119	1.028	0.919	0.0367	33.839
0.793	1.174	1.131	0.963	0.0164	104.087
1.427	1.526	1.205	0.790	0.1024	8.305
1.436	1.543	1.310	0.849	0.0711	13.733
1.418	1.564	1.407	0.900	0.0458	25.005
1.377	1.595	1.498	0.939	0.0273	51.220
1.241	1.638	1.597	0.975	0.0110	175.371

A logarithmic plot of the submerged-flow data is shown in Figure 6. Each data point in Figure 12 can have a line drawn at a slope on n_f = 1.55, which can be extended to where it intercepts the abscissa at $h_u - h_d = 1.0$; then, the corresponding value of discharge can be read on the ordinate, which is listed as $Q_{\Delta h = 1.0}$ in Table 5. The value of $Q_{\Delta h = 1.0}$ can also be solved analytically because a straight line on logarithmic paper is a power function having the simple form:

$$Q_s = Q_{\Delta h = 1.0} (h_u - h_d)^{n_f} \tag{11}$$

or

$$Q_{\Delta h=1.0} = \frac{Q_s}{(h_u - h_d)^{n_f}} \tag{12}$$

where $Q_{\Delta h = 1.0}$ has a different value for each value of the submergence, S.

Using the term $Q_{\Delta h = 1.0}$, implies that $h_u - h_d = 1.0$ by definition, so that Equation 10 reduces to:

$$Q_{\Delta h=1.0} = \frac{C_s(1.0)^{n_f}}{(-\log S)^{n_s}} = C_s(-\log S)^{-n_s} \tag{13}$$

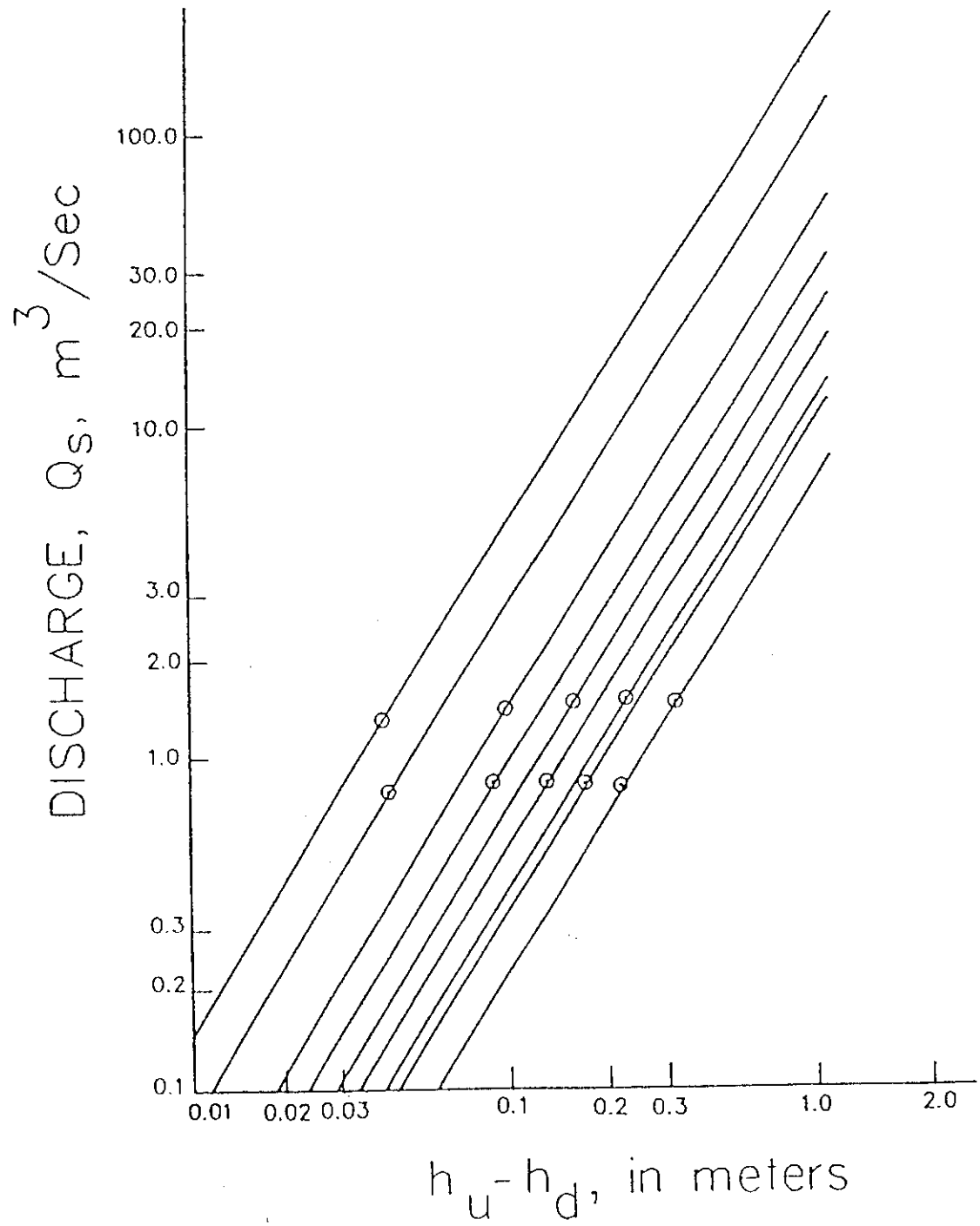

Figure 6. Logarithmic plot of submerged-flow data for the example open-channel constriction.

Again, this is a power function where $Q_{\Delta h = 1.0}$ can be plotted against (-logS) on logarithmic paper to yield a straight line relationship. The submerged-flow data in Table 5 is plotted in Figure 7. Note that the straight line has a negative slope ($-n_s$) and that C_s is the value of $Q_{\Delta h = 1.0}$ when (-logS) is equal to 1.0. For this particular data, the submerged-flow equation is:

$$Q_s = \frac{0.367(h_u - h_d)^{1.55}}{(-logS)^{1.37}} \qquad (14)$$

By setting the free-flow discharge equation equal to the submerged-flow discharge equation (Equations 7 and 14), the transition submergence, S_t, can be determined:

$$0.74h_u^{1.55} = \frac{0.367(h_u - h_d)^{1.55}}{(-logS)^{1.37}} \qquad (15)$$

and,

$$0.74(-logS)^{1.37} = 0.367(1-S)^{1.55} \qquad (16)$$

The value of S in this relationship is S_t provided the coefficients and exponents have been accurately determined. Again, small errors will dramatically affect the determination of S_t.

$$0.74(-logS_t)^{1.37} = 0.367(1-S_t)^{1.55} \qquad (17)$$

Equation 17 is solved by trial-and-error to determine S_t, which in this case is 0.82. Thus, free flow exists when $S < 0.82$ and submerged flow exists when the submergence is greater than 82 percent.

A final free-flow and submerged-flow discharge rating is plotted on logarithmic paper in Figure 8. Also, Table 6 is a typical free-flow rating based on Equation 7 for the example open-channel constriction. The submerged-flow discharge can be calculated using the reduction factors in Table 7 to multiply by the free-flow rating corresponding to the measured value of h_u. This reduction factor is obtained by calculating the ration Q_s/Q_f:

$$\frac{Q_s}{Q_f} = \frac{0.367(h_u - h_d)^{1.55}}{(-logS)^{1.37}} \frac{1}{0.74h_u^{1.55}} \qquad (18)$$

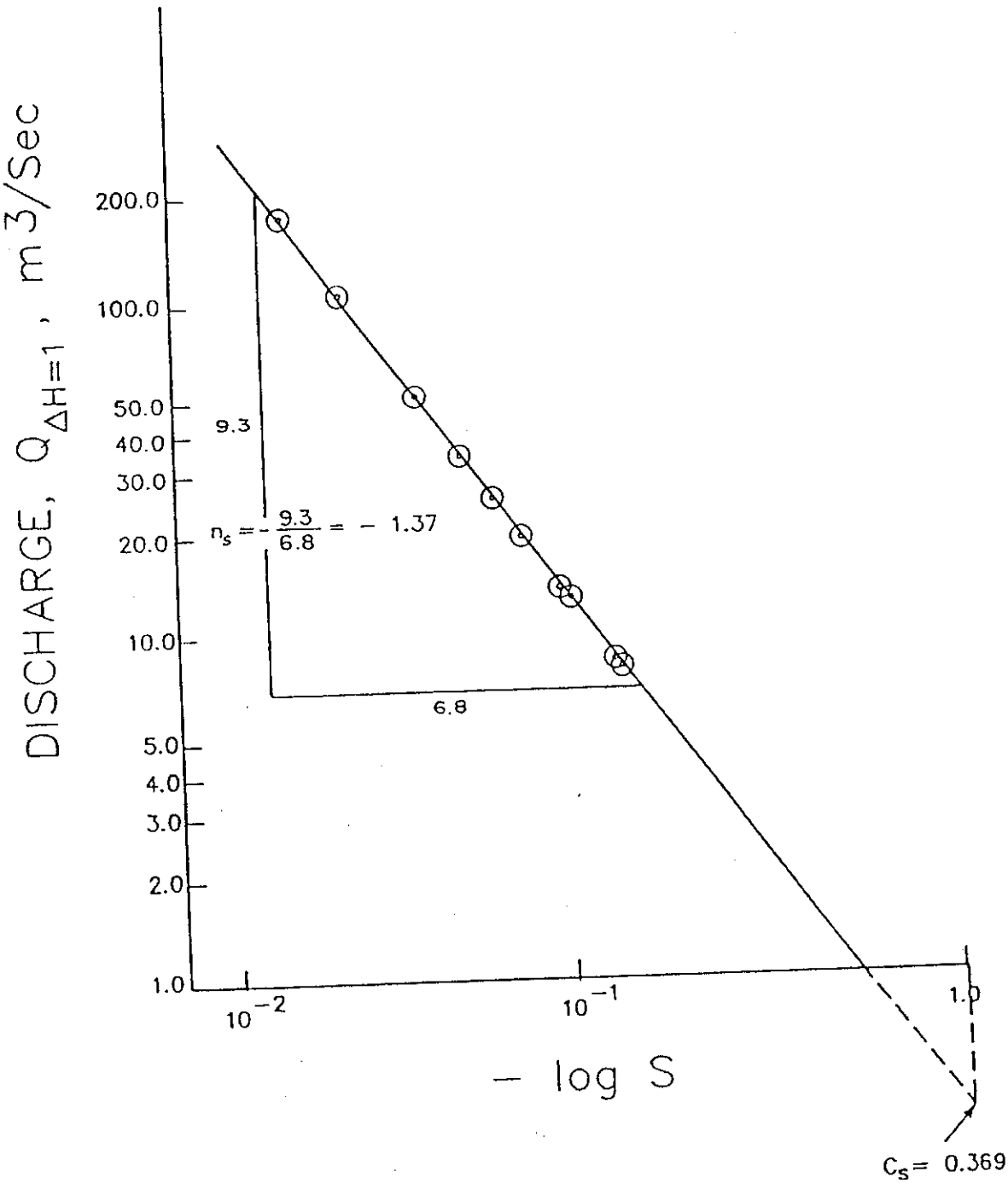

Figure 7. Logarithmic plot for determining the submerged-flow coefficient, C_s, and the submerged-flow exponent, n_s, for the example open-channel constriction.

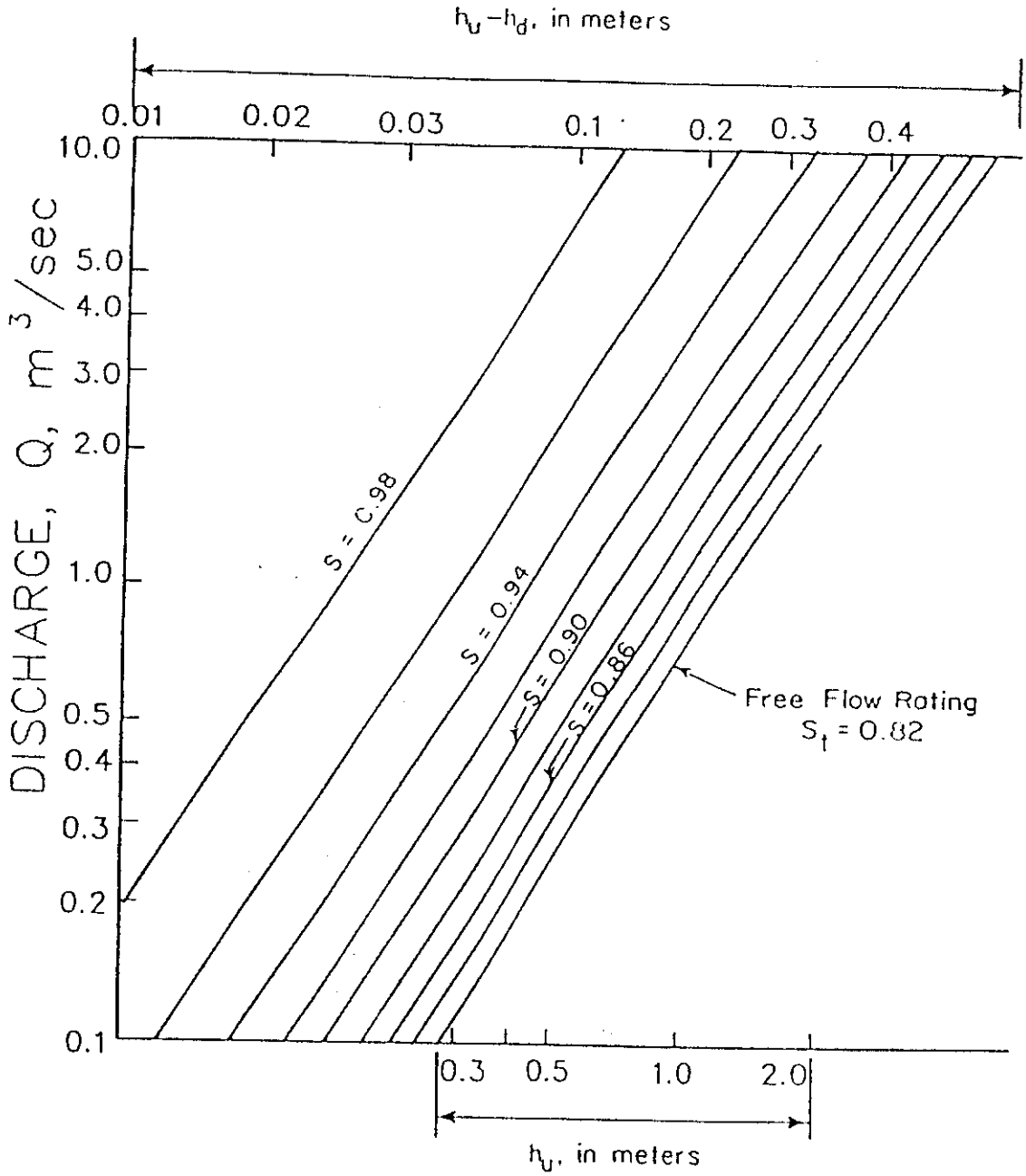

Figure 8. Free-flow and submerged-flow rating for the example open-channel constriction.

TABLE 6. Free-flow discharge rating for example open-channel constriction.

h_v m	Q_f m³/s	h_v m	Q_f m³/s	h_v m	Q_f m³/s	h_v m	Q_f m³/s
0.810	0.534	1.110	0.870	1.410	1.260	1.710	1.700
0.820	0.544	1.120	0.882	1.420	1.274	1.720	1.715
0.830	0.554	1.130	0.894	1.430	1.288	1.730	1.731
0.840	0.565	1.140	0.907	1.440	1.302	1.740	1.746
0.850	0.575	1.150	0.919	1.450	1.316	1.750	1.762
0.860	0.586	1.160	0.931	1.460	1.330	1.760	1.777
0.870	0.596	1.170	0.944	1.470	1.345	1.770	1.793
0.880	0.607	1.180	0.956	1.480	1.359	1.780	1.809
0.890	0.618	1.190	0.969	1.490	1.373	1.790	1.825
0.900	0.629	1.200	0.982	1.500	1.387	1.800	1.840
0.910	0.639	1.210	0.994	1.510	1.402	1.810	1.856
0.920	0.650	1.220	1.007	1.520	1.416	1.820	1.872
0.930	0.661	1.230	1.020	1.530	1.431	1.830	1.888
0.940	0.672	1.240	1.033	1.540	1.445	1.840	1.904
0.950	0.683	1.250	1.046	1.550	1.460	1.850	1.920
0.960	0.695	1.260	1.059	1.560	1.474	1.860	1.936
0.970	0.706	1.270	1.072	1.570	1.489	1.870	1.952
0.980	0.717	1.280	1.085	1.580	1.504	1.880	1.969
0.990	0.729	1.290	1.098	1.590	1.518	1.890	1.985
1.000	0.740	1.300	1.111	1.600	1.533	1.900	2.001
1.010	0.752	1.310	1.125	1.610	1.548	1.910	2.018
1.020	0.763	1.320	1.138	1.620	1.563	1.920	2.034
1.030	0.775	1.330	1.151	1.630	1.578	1.930	2.050
1.040	0.786	1.340	1.165	1.640	1.593	1.940	2.067
1.050	0.798	1.350	1.178	1.650	1.608	1.950	2.083
1.060	0.810	1.360	1.192	1.660	1.623	1.960	2.100
1.070	0.822	1.370	1.205	1.670	1.638	1.970	2.117
1.080	0.834	1.380	1.219	1.680	1.654	1.980	2.133
1.090	0.846	1.390	1.233	1.690	1.669	1.990	2.150
1.100	0.858	1.400	1.247	1.700	1.684	2.000	2.167

TABLE 7. Submerged-flow reduction factors for the example open-channel constriction.

S	Q_s/Q_f	S	Q_s/Q_f
0.82	1.000	0.91	0.9455
0.83	0.9968	0.92	0.9325
0.84	0.9939	0.93	0.9170
0.85	0.9902	0.94	0.8984
0.86	0.9856	0.95	0.8757
0.87	0.9801	0.96	0.8472
0.88	0.9735	0.97	0.8101
0.89	0.9657	0.98	0.7584
0.90	0.9564	-	-

Which is also equal to

$$\frac{Q_s}{Q_f} = \frac{0.496(1-S)^{1.55}}{(-\log S)^{1.37}} \qquad (19)$$

For example, if h_u and h_d are measured and found to be 1.430 and 1.337, the first step would be to compute the submergence, S,

$$S = \frac{1.337}{1.430} = 0.935 \qquad (20)$$

Thus, the submerged-flow condition exists in the example open-channel constriction. From Table 6, the value of Q_f is 1.288 m^3/s for h_u = 1.430 m. Then, entering Table 7, the value of Q_s/Q_f can be found by interpolating halfway between S = 0.93 and S = 0.94. Thus, Q_s/Q_f= 0.9077. Consequently, Q_s can be determined from

$$Q_s = Q_f\left(\frac{Q_s}{Q_f}\right) = 1.288(0.9077) = 1.169 m^3/s \qquad (21)$$

Finally, it should be noted that all of the preceding graphical solutions to the calibration of open-channel constrictions can also be obtained numerically through logarithmic transformations and linear regression. The graphical solutions have the advantage of being more didactic; however, for experienced persons, the numerical solution is usually more convenient. It is always useful to plot the results, either by hand or using computer software, to reduce the possibility of errors or inclusion of erroneous data values. Obvious errors tend to be more apparent in plots than in numerical calibration results.

2.4. Rating Orifices

Any type of opening in which the upstream water level is higher than the top of the opening is referred to as an orifice. In this case, if the jet of water emanating from the orifice discharges freely into the air or downstream channel without backwater or tailwater effect, then the orifice is operating under free-flow conditions. If the upstream water level is below the top of the opening, then the opening is hydraulically performing as a weir structure. For free-flow conditions through an orifice, the discharge equation is:

$$Q_f = C_d\, C_v\, A\, \sqrt{2gh_u} \qquad (22)$$

where C_d is the dimensionless discharge coefficient, C_v is the dimensionless velocity head coefficient, A is the cross-sectional area of the orifice opening, g is the acceleration due to gravity, and h_u is measured from the centroid of the orifice to the upstream water level as shown in Figure 9a.

The upstream depth, h_u, can also be measured from the bottom of the orifice opening if the downstream depth is taken to be about 0.611 times the vertical orifice opening, which takes into account the theoretical flow contraction just downstream of the orifice. Otherwise, the inferred assumption is that the downstream depth is equal to one-half the opening, and h_u is effectively measured from the area centroid of the opening. Either of these two assumptions may be adequate in rating the orifice for free-flow conditions, and in defining the governing equation, but it should be noted that the choice will affect the value of the discharge coefficient.

If the downstream water level is also above the top of the orifice (see Figure 9b), then submerged conditions exist and the discharge equation becomes:

$$Q_s = C_d\, C_v\, A\, \sqrt{2g(h_u - h_d)} \qquad (23)$$

Where $h_u - h_d$ is the difference in water surface elevations upstream and downstream of the submerged orifice.

The velocity head coefficient, C_v, approaches unity as the approach velocity to the orifice decreases to zero. In irrigation systems, C_v can usually be assumed to be unity since most irrigation channels have very flat gradients and the flow velocities are low (usually much less than 1 m/s).

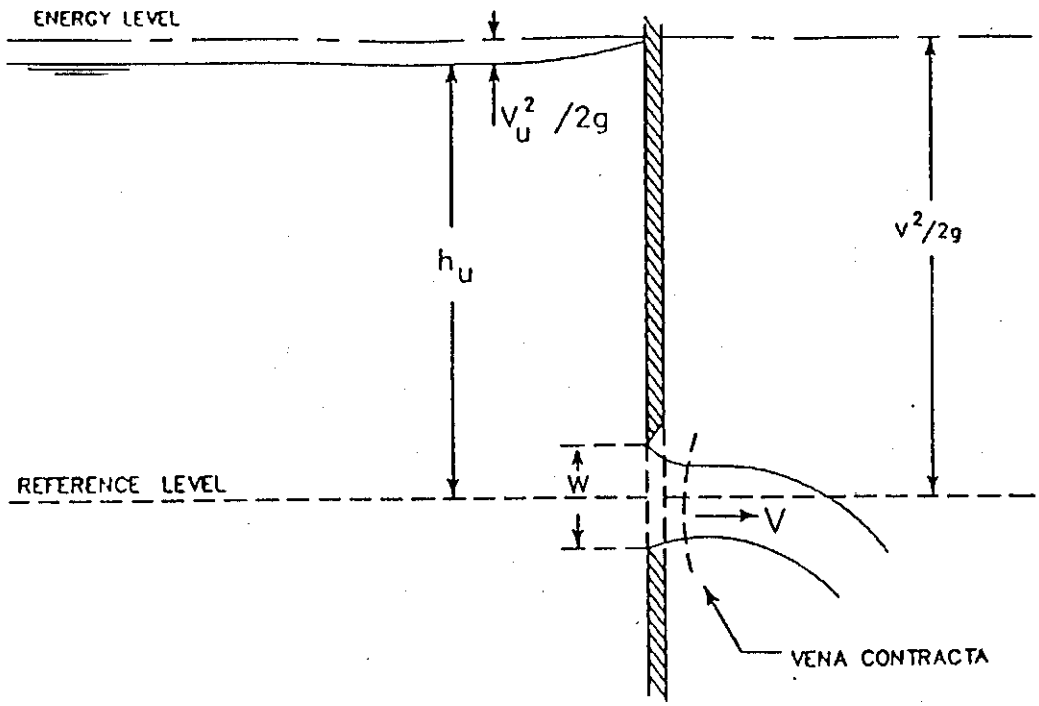

(a) FREE FLOW

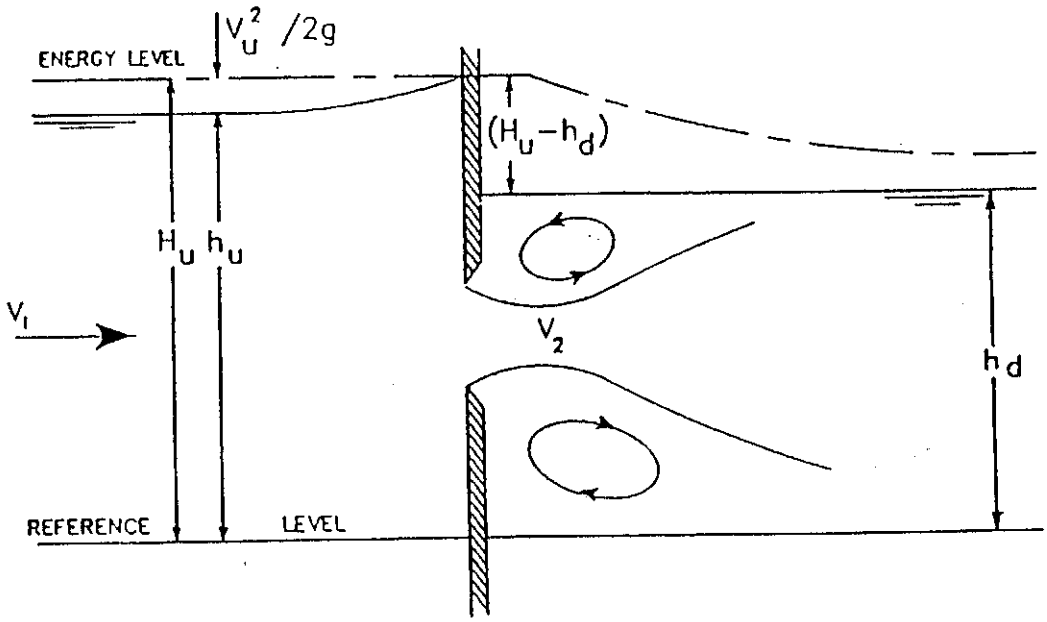

(b) SUBMERGED FLOW

Figure 9. Definition sketch of orifice flow.

An orifice can be used as a highly accurate flow measuring device in an irrigation system. If the orifice structure has not been previously rated in the laboratory, then it can easily be rated in the field. The hydraulic head term, h_u, or $(h_u - h_d)$, can be relied upon to have the exponent 1/2, which means that a single field rating measurement, if accurately made, will provide an accurate determination of the coefficient of discharge, C_d. However, the use of a single rating measurement implies the assumption of a constant C_d value, which is not the case in general. Adjustments to the basic orifice equations for free- and submerged-flow are often made to more accurately represent the structure rating as a function of flow depths and gate openings. The following sections present some alternative equation forms for taking into account the variability in the discharge coefficient under different operating conditions. Orifices usually have C_d values of about 0.60 to 0.80, depending on the geometry and installation of the structure, but values ranging from about 0.3 to 0.9 have been measured in the field.

2.4.1 Free-Flow Rectangular Gate Structures

A definition sketch for a rectangular gate structure having free orifice flow is shown in Figure 10. For a rectangular gate having a gate opening, G_o, and a gate width, W, the free-flow discharge equation can be obtained from Equation 22, assuming that the dimensionless velocity head coefficient is unity.

$$Q_f = C_d\, G_o\, W\sqrt{2g(h_u - G_o/2)} \qquad (24)$$

where G_o is the vertical gate opening, W is the gate width, and G_oW is the area, A, of the orifice opening.

The upstream flow depth, h_u, can be measured anywhere upstream of the gate, including the upstream face of the gate. The value of h_u will vary a small amount depending on the location chosen for measuring h_u. Consequently, the value of the coefficient of discharge, C_d, will also vary according to the location selected for measuring h_u.

One of the most difficult tasks in calibrating a gate structure is obtaining a highly accurate measurement of the gate opening, G_o. For gates having a threaded rod that rises as the gate opening is increased, the gate opening is read from the top of the handwheel to the top of the rod with the gate closed, and then set at some opening, G_o. This very likely represents a measurement of gate opening from where the gate is totally seated, rather than a measurement from the gate sill; therefore, the measured value of G_o from the threadrod will usually be greater than the true gate opening, unless special precautions (described below) are taken to calibrate the threadrod.

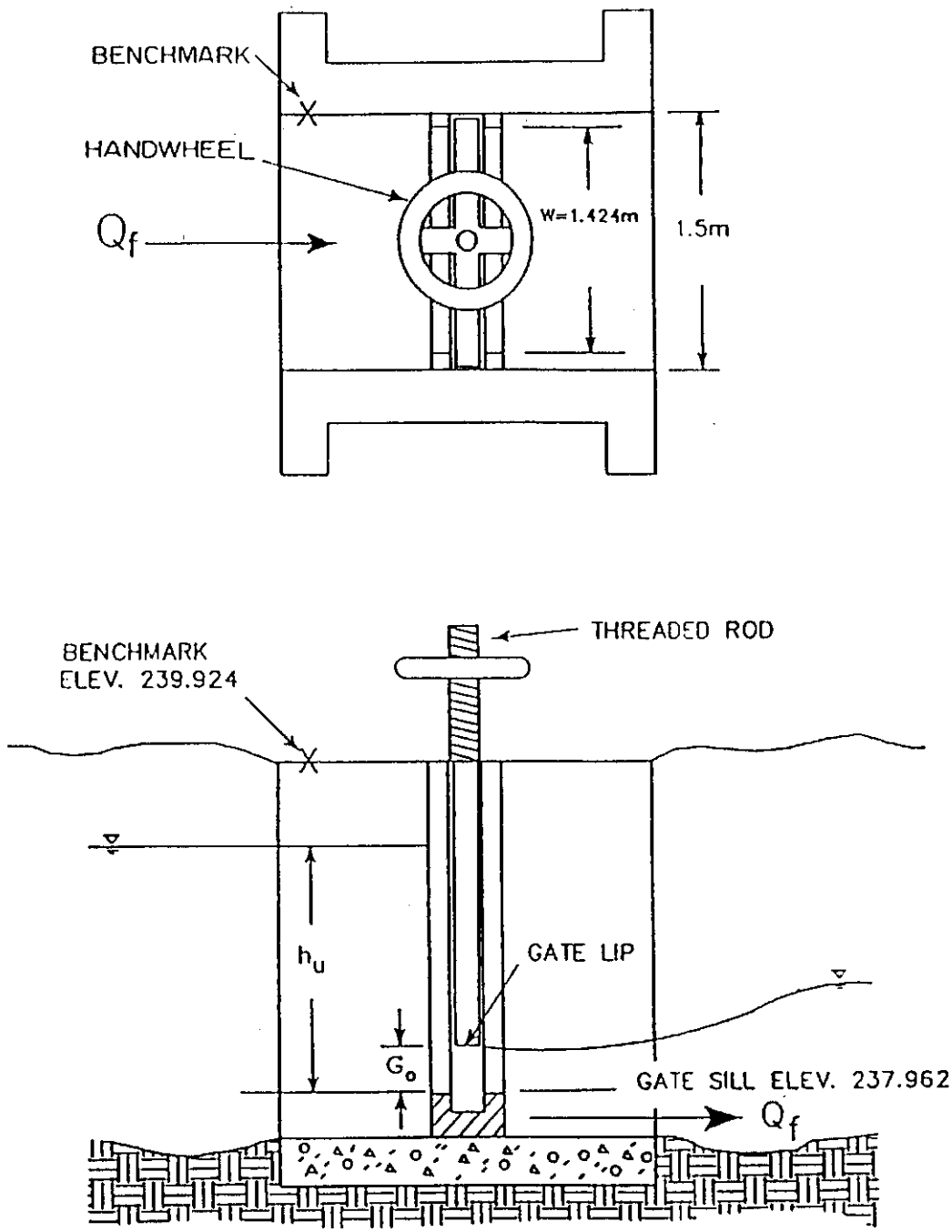

Figure 10. Definition sketch and example problem for a rectangular gate structure having free-orifice flow.

Likewise, when the gate lip is set at the same elevation as the gate sill, there will undoubtedly be some flow or leakage through the gate. This implies that the datum for measuring the gate opening is below the gate sill. In fact, there is often leakage from a gate even when it is totally seated (closed) because of inadequate maintenance. An example problem will be used to illustrate the procedure for determining an appropriate zero datum for the gate opening.

For the rectangular gate structure shown in Figure 10, the calibration data listed in Table 8 was collected. The data reduction is listed in Table 9 where the coefficient of discharge, C_d, was calculated from Equation 24.

A rectangular coordinate plot of C_d versus the gate opening, G_o, listed in Table 9 is shown graphically in Figure 11. The value of C_d continues to decrease with larger gate openings. To determine if a constant value of C_d can be derived, Equation 24 can be rewritten in the following format:

$$Q_f = C_d(G_o+\Delta G_o)\, W \sqrt{2g\left((h_u)_{\Delta G_o} - \frac{G_o + \Delta G_o}{2}\right)} \qquad (25)$$

Where ΔG_o is a measure of the zero datum level below the gate sill, which

$$(h_u)_{\Delta G_o} = h_u + \Delta G_o \qquad (26)$$

is shown in Figure 12. An appropriate value of ΔG_o will be determined by trial-and error for the example problem. Assuming values of ΔG_o equal to 1 mm, 2 mm, 3 mm, etc., the computations for determining C_d can be made using Equation 25. The results for ΔG_o equal to 1 mm, 2 mm, 3 mm, 4 mm, 5 mm, 6 mm, 7 mm, 8 mm and 12 mm (gate seated) are listed in Table 10. The best results are obtained from ΔG_o of 3 mm; this result is plotted in Figure 13, which shows that C_d varies from 0.582 to 0.593 with the average value of C_d being 0.587. For this particular gate structure, the discharge normally varies between 200 and 300 lps, and the gate opening is normally operated between 40-60 mm, so that a constant value of C_d = 0.587 can be used when the zero datum for G_o and h_u is taken as 3 mm below the gate sill (another alternative would be to use a constant value of C_d = 0.575 for ΔG_o = 4 mm and G_o greater than 30 mm).

TABLE 8. Example of field calibration data for a rectangular gate structure having free orifice flow.

Discharge, Q_f m^3/s	Gate Opening, G_o m	Upstream Benchmark Tape Measurement m
0.0646	0.010	0.124
0.0708	0.020	1.264
0.0742	0.030	1.587
0.0755	0.040	1.720
0.0763	0.050	1.787
0.0767	0.060	1.825

TABLE 9. Data reduction for example rectangular gate structure having free orifice flow.

Q_f m^3/s	G_o m	h_u m	C_d (see note below)
0.0646	0.010	1.838	0.756
0.0708	0.020	0.698	0.677
0.0742	0.030	0.375	0.654
0.0755	0.040	0.242	0.635
0.0763	0.050	0.175	0.625
0.0767	0.060	0.137	0.620

Note: The discharge coefficient, C_d, was calculated using the following equation:

$$Q_f = C_d G_o W\sqrt{2g\,(h_u - G_o/2)}$$

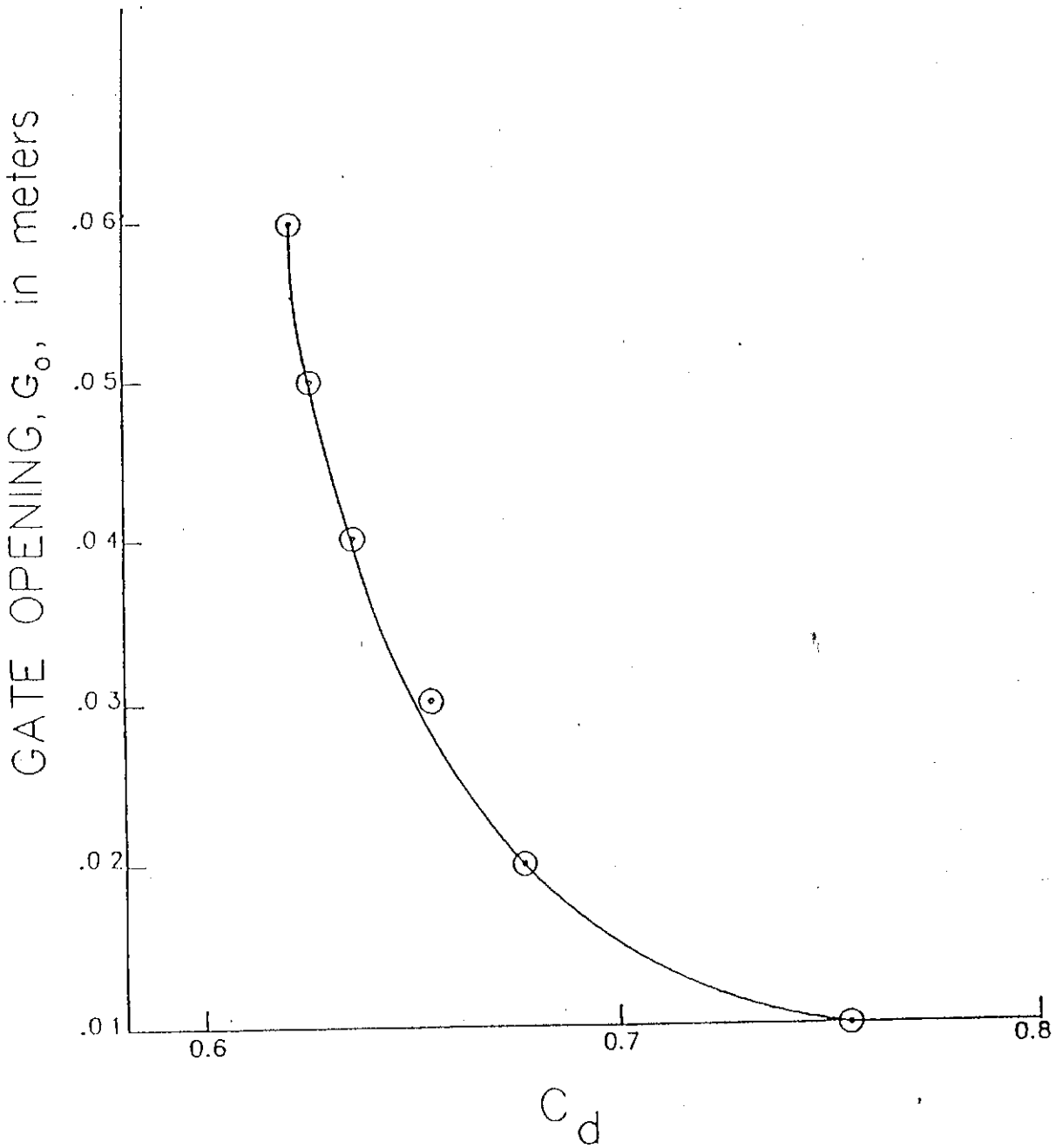

Figure 11. Variation in the discharge coefficient, C_d, with gate opening, G_o, for the example rectangular gate structure with free orifice flow.

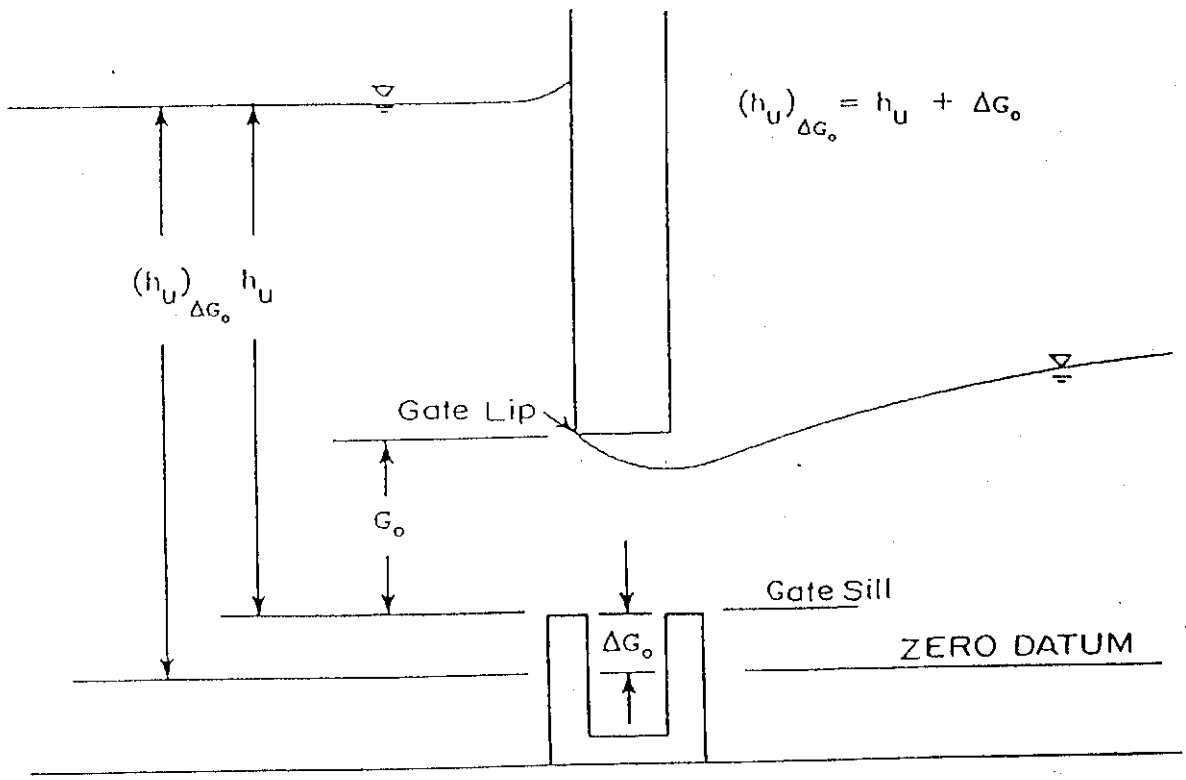

Figure 12. Definition sketch of the zero datum level for gate opening and upstream flow depth for a rectangular gate structure.

TABLE 10. Computation of the discharge coefficient, C_d, for adjusted values of gate opening and upstream flow depth for the example rectangular gate structure having free orifice flow.

Q_f m^3/s	G_o m	h_u m	Discharge Coefficient, C_d (see note below)									
			ΔG_o 0 mm	ΔG_o 1 mm	ΔG_o 2 mm	ΔG_o 3 mm	ΔG_o 4 mm	ΔG_o 5 mm	ΔG_o 6 mm	ΔG_o 7 mm	ΔG_o 8 mm	ΔG_o 12mm
0.0646	0.010	1.838	0.756	0.688	0.630	0.582	0.540	0.504	0.472	0.445	0.420	0.344
0.0708	0.020	0.698	0.677	0.644	0.615	0.588	0.563	0.540	0.519	0.500	0.482	0.425
0.0742	0.030	0.375	0.654	0.632	0.612	0.593	0.575	0.558	0.542	0.527	0.513	0.471
0.0755	0.040	0.242	0.635	0.619	0.604	0.589	0.575	0.561	0.549	0.536	0.525	0.495
0.0763	0.050	0.175	0.625	0.611	0.599	0.586	0.575	0.563	0.552	0.542	0.531	0.514
0.0767	0.060	0.137	0.620	0.608	0.597	0.586	0.575	0.565	0.556	0.546	0.537	0.531

Note: The last colum with ΔG_o = 12 mm is for the gate totally seated (closed). The discharge coefficient, C_d, was calculated from:

$$Q_f = C_d (G_o + \Delta G_o) W \sqrt{2g \left((h_u)_{\Delta G_o} - \frac{G_o + \Delta G_o}{2} \right)}$$

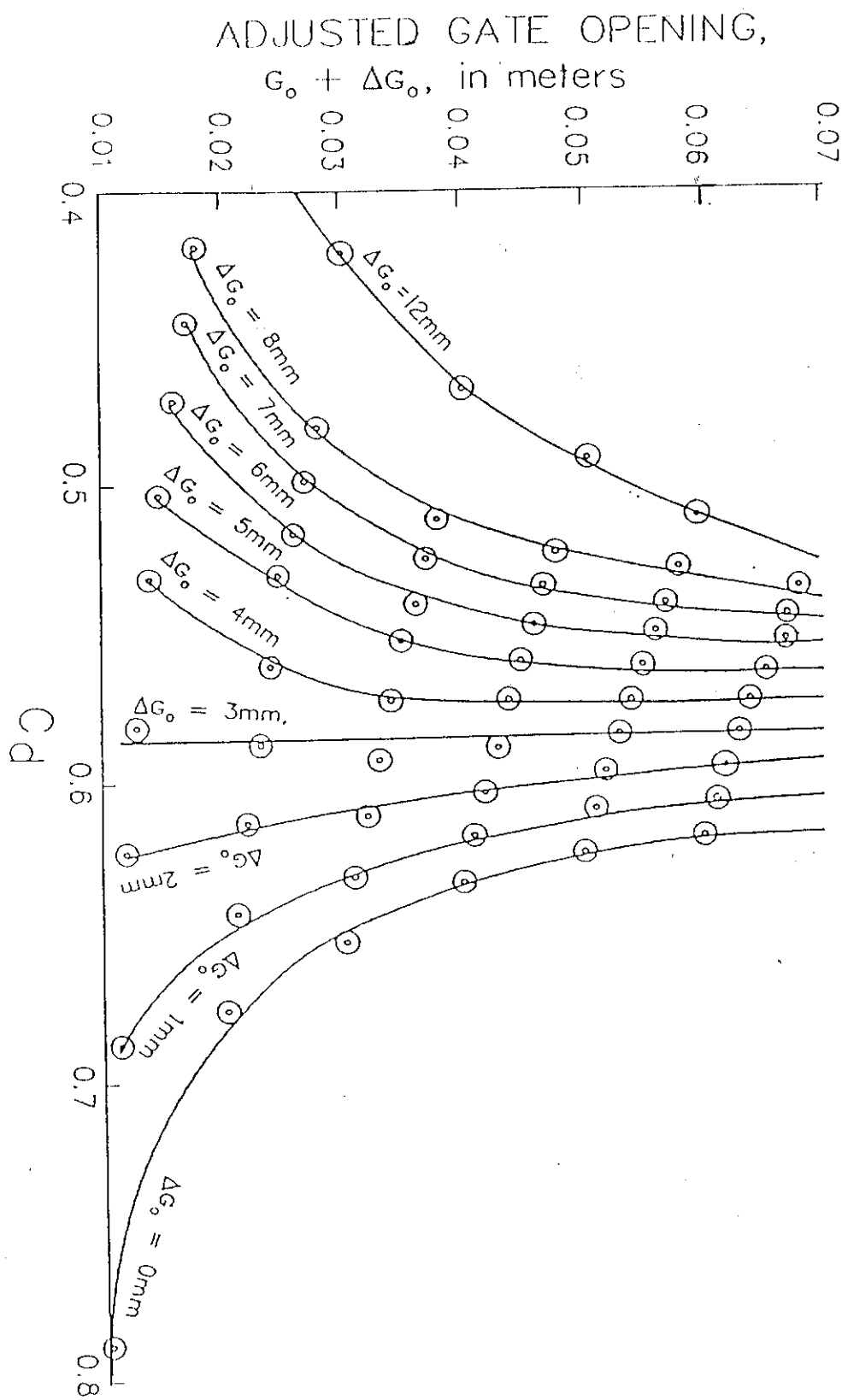

Figure 13. Variation in the discharge coefficient, C_d, with the adjusted gate opening, $G_o + \Delta G_o$, for the example rectangular gate structure with free orifice flow.

2.4.2 Submerged-Flow Rectangular Gate Structures

Submerged-flow gate structures are the most common constrictions employed in irrigation networks. The gates are used to regulate the water levels upstream and the discharge downstream. For this reason, they are very important structures that need to be field calibrated. Fortunately, they are one of the easiest structures to field calibrate for discharge measurement.

A definition sketch for a rectangular gate structure having submerged orifice flow is shown in Figure 14. Assuming that the dimensionless velocity head coefficient in Equation 23 is unity, the submerged-flow discharge equation for a rectangular gate having an opening G_o, and a width, W, becomes:

$$Q_s = C_d\, G_o\, W\sqrt{2g\,(h_u - h_d)} \qquad (27)$$

where G_oW is the area, A, of the orifice.

The upstream flow depth, h_u, can be measured anywhere upstream of the gate, including the upstream face of the gate. Likewise, the downstream flow depth, h_d, can be measured anywhere downstream of the gate, including the downstream face of the gate. Many times, h_u and h_d will be measured at the gate because only one reference benchmark is needed on top of the gate structure in order to make tape measurements down to the water surface. This is satisfactory if the water surfaces on the gate are smooth. If not, h_u and h_d should be measured at locations where the water surface is smooth, not turbulent and fluctuating.

All of the information in the previous section regarding the measurement of gate opening, G_o , applies equally well for submerged gates.

For the rectangular gate structure shown in Figure 14, the field calibration data is listed in Table 11. Note that for this type of slide gate, the gate opening was measured both on the left side $(G_o)_L$, and the right side, $(G_o)_R$, because the gate lip is not always horizontal. The data reduction is listed in Table 12 where the coefficient of discharge, C_d, was calculated from Equation 27. The variation in C_d with gate opening, G_o, is plotted in Figure 15.

As in the case of the free-flow orifice calibration in the previous section, a trial-and-error approach can be used to determine a more precise zero datum for the gate opening (see Figure 12). In this case, Equation 27 would be rewritten as:

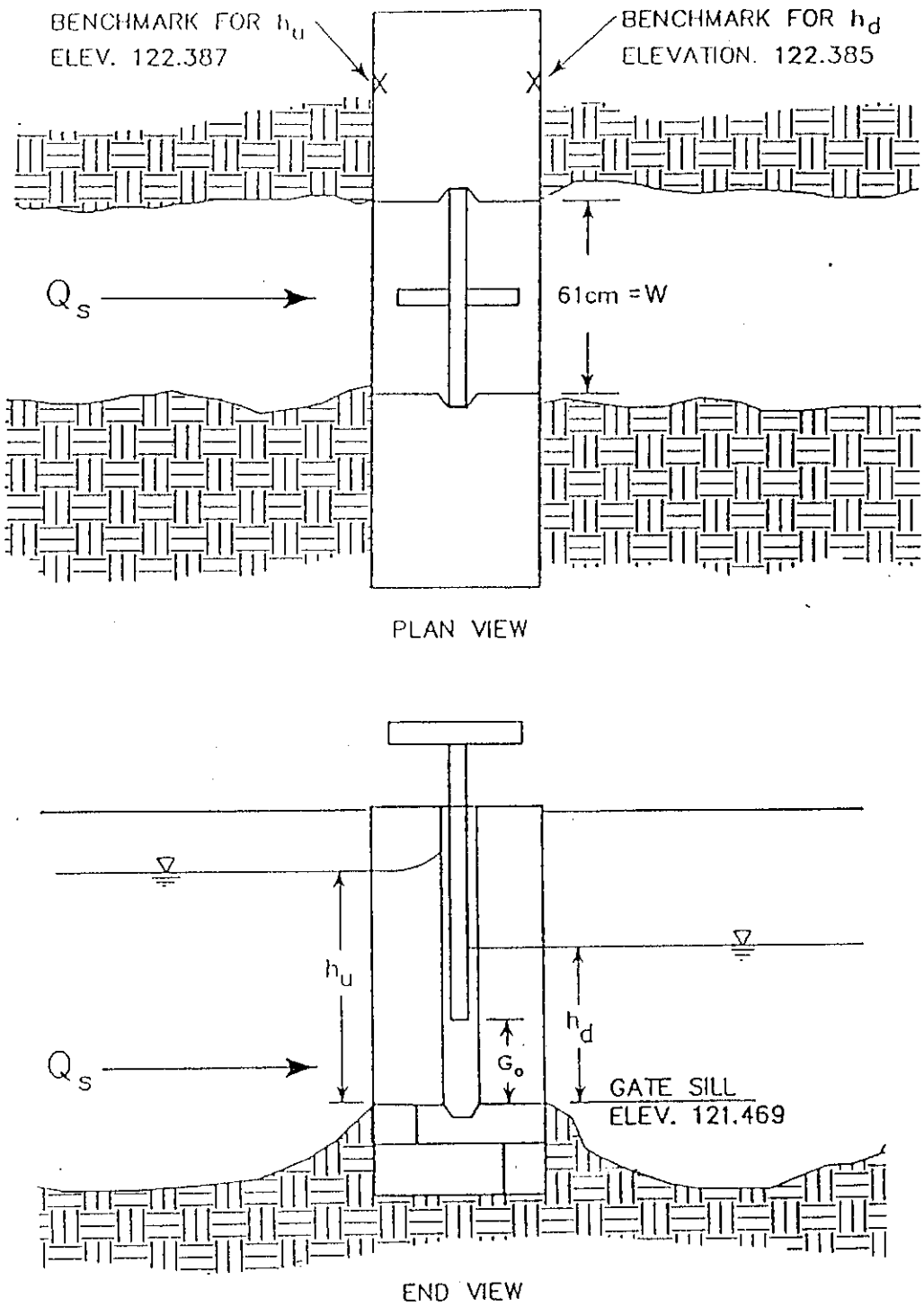

Figure 14. Definition sketch and example problem for a rectangular gate structure having submerged orifice flow.

Next >>